

## Prediction of particulate fouling in full-scale reverse osmosis plants using the modified fouling index – ultrafiltration (MFI-UF) method

Abunada, Mohanad; Dhakal, Nirajan; Gulrez, Raffay; Li, Yuke; Abushaban, Almotasembellah; Smit, Herman; Moed, David; Ghaffour, Noreddine; Kennedy, Maria D.; More Authors

**DOI**

[10.1016/j.desal.2023.116478](https://doi.org/10.1016/j.desal.2023.116478)

**Publication date**

2023

**Document Version**

Final published version

**Published in**

Desalination

**Citation (APA)**

Abunada, M., Dhakal, N., Gulrez, R., Li, Y., Abushaban, A., Smit, H., Moed, D., Ghaffour, N., Kennedy, M. D., & More Authors (2023). Prediction of particulate fouling in full-scale reverse osmosis plants using the modified fouling index – ultrafiltration (MFI-UF) method. *Desalination*, 553, Article 116478. <https://doi.org/10.1016/j.desal.2023.116478>

**Important note**

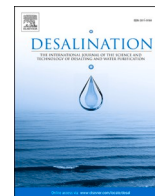
To cite this publication, please use the final published version (if applicable).  
Please check the document version above.

**Copyright**

Other than for strictly personal use, it is not permitted to download, forward or distribute the text or part of it, without the consent of the author(s) and/or copyright holder(s), unless the work is under an open content license such as Creative Commons.

**Takedown policy**

Please contact us and provide details if you believe this document breaches copyrights.  
We will remove access to the work immediately and investigate your claim.



## Prediction of particulate fouling in full-scale reverse osmosis plants using the modified fouling index – ultrafiltration (MFI-UF) method

Mohanad Abunada<sup>a,b,\*</sup>, Nirajan Dhakal<sup>a</sup>, Raffay Gulrez<sup>a</sup>, Pamela Ajok<sup>a</sup>, Yuke Li<sup>a</sup>, Almotasembellah Abushaban<sup>c</sup>, Herman Smit<sup>d</sup>, David Moed<sup>e</sup>, Noreddine Ghaffour<sup>f</sup>, Jan C. Schippers<sup>a</sup>, Maria D. Kennedy<sup>a,b</sup>

<sup>a</sup> IHE-Delft Institute for Water Education, Water Supply, Sanitation and Environmental Engineering Department, Westvest 7, 2611 AX Delft, the Netherlands

<sup>b</sup> Delft University of Technology, Faculty of Civil Engineering, Stevinweg 1, 2628 CN Delft, the Netherlands

<sup>c</sup> Mohammed VI Polytechnic University, International Water Research Institute, Lot 660, Hay Moulay Rachid, Ben Guerir 43150, Morocco

<sup>d</sup> PWN, Rijksweg 501, 1991 AS Velsbroek, the Netherlands

<sup>e</sup> Evides Industriewater, 3006 AL Rotterdam, the Netherlands

<sup>f</sup> Water Desalination and Reuse Center (WDRC), Biological and Environmental Science and Engineering (BESE) Division, King Abdullah University of Science and Technology (KAUST), Thuwal 23955-6900, Saudi Arabia

### HIGHLIGHTS

- MFI-UF method was used to predict particulate fouling rate in full-scale RO plants.
- 10–100 kDa UF membranes can be used in MFI-UF test to predict particulate fouling.
- The variation between the predicted and actual fouling rates in RO plants was <15 %.
- Accuracy of fouling prediction depends highly on the flux consistency in RO plants.

### ARTICLE INFO

#### Keywords:

Reverse osmosis (RO)  
Particulate fouling prediction  
MFI-UF  
Particle deposition factor  
Membrane surface porosity correction

### ABSTRACT

This study aims at applying and verifying the MFI-UF method to predict particulate fouling in RO plants. Two full-scale RO plants treating surface water, with average capacity of 800–2000 m<sup>3</sup>/h, were studied. Firstly, the MFI-UF of RO feed and concentrate was measured using 5–100 kDa membranes at same flux applied in the RO plants (20–26 L/m<sup>2</sup>.h). Subsequently, the particle disposition factor ( $\Omega$ ) was calculated to simulate particle deposition in RO cross-flow filtration. Finally, particulate fouling rates were predicted based on MFI-UF and  $\Omega$ , and compared with the actual fouling rates in the plants. For plant A, the results showed that the fouling rates predicted using MFI-UF measured with 100 kDa membrane have the best agreement with the actual fouling (with 3–11 % deviation). For plant B, the fouling rates predicted based on both 10 and 100 kDa membranes agree well with the actual fouling (with 2 % and 15 % deviation, respectively). However, the fouling predicted based on 5 kDa membrane is considerably overestimated for both plants, which is attributed to the effect of the low surface porosity of 5 kDa membrane. More widespread applications of MFI-UF in full-scale RO plants are required to demonstrate the most suitable MFI-UF membranes for fouling prediction.

### 1. Introduction

Reverse osmosis (RO) technology has been rapidly growing in the water treatment sector due to the continuous advancements in both design and operation [1]. However, RO membrane fouling still remains

a key challenge. Fouling can cause a decline in the RO membrane permeability. Consequently, higher energy and more frequent membrane cleaning are required to maintain water production, which eventually results in increased O&M costs.

Particulate fouling, due to the deposition of particles and colloids on the membrane, is one of the types of fouling which is persistently

\* Corresponding author at: IHE-Delft Institute for Water Education, Water Supply, Sanitation and Environmental Engineering Department, Westvest 7, 2611 AX Delft, the Netherlands.

E-mail addresses: [m.b.m.abunada@tudelft.nl](mailto:m.b.m.abunada@tudelft.nl), [m.abunada@un-ihe.org](mailto:m.abunada@un-ihe.org) (M. Abunada).

<https://doi.org/10.1016/j.desal.2023.116478>

Received 15 November 2022; Received in revised form 10 February 2023; Accepted 12 February 2023

Available online 22 February 2023

0011-9164/© 2023 The Authors. Published by Elsevier B.V. This is an open access article under the CC BY-NC-ND license (<http://creativecommons.org/licenses/by-nc-nd/4.0/>).

### Nomenclature

|                     |  |
|---------------------|--|
| $MFI-UF$            | Modified fouling index – ultrafiltration [ $s/L^2$ ]             |
| $I$                 | Fouling index [ $1/m^2$ ]  |
| $J$                 | Flux [ $L/m^2 \cdot h$ or $m^3/m^2 \cdot s$ ]                    |
| $\Delta P$          | Transmembrane pressure [bar or Pa]                               |
| $R_m$               | Clean membrane resistance [ $1/m$ ]                              |
| $R_c$               | Cake resistance [ $1/m$ ]  |
| $\eta$              | Feed water viscosity [ $N \cdot s/m^2$ ]                         |
| $t$                 | Filtration time [s, min, h, day, or month]                       |
| $\Delta P_o$        | Reference transmembrane pressure [= 2 bar or 200 kPa]            |
| $\eta_{20^\circ C}$ | Reference water viscosity at 20 °C [= 0.001002 $N \cdot s/m^2$ ] |
| $A_o$               | Reference MFI membrane surface area [= 0.00138 $m^2$ ]           |
| $NDP$               | Net driving pressure [bar]                                       |
| $\Delta NDP$        | Differential net driving pressure [bar]                          |
| $\Omega$            | Particle deposition factor [–]                                   |
| $R$                 | RO recovery (ratio of RO permeate flow to RO feed flow) [–]      |
| $P_f$               | RO feed pressure [bar or Pa]                                     |
| $P_p$               | RO permeate pressure [bar or Pa]                                 |
| $dP$                | Pressure drop across the RO membrane [bar or Pa]                 |
| $\Delta P_{osm}$    | Differential osmotic pressure across the RO membrane [bar or Pa] |
| $T$                 | RO feed temperature (°C)   |

experienced in RO plants. Therefore, there is a need for a reliable method which can accurately measure and predict the particulate fouling potential of RO feed water, allowing the performance of RO plants to be assessed and monitored. The existing ASTM standard assessment methods; silt density index (SDI) [2] and modified fouling index (MFI-0.45) [3], simulate particulate fouling using a 0.45  $\mu m$  membrane. Thus, the effect of small colloids ( $< 0.45 \mu m$ ), which are more likely to be responsible for RO membrane fouling, is not evaluated in either method [4]. Consequently, a more promising method; the modified fouling index – ultrafiltration (MFI-UF) was developed, whereby a UF membrane is used in order to capture smaller colloids [5–9]. The MFI-UF was performed initially at constant pressure (as is the MFI-0.45/SDI). Later, the method was developed further to be measured at constant flux in order to simulate the operation of RO plants in practice [10,11]. Furthermore, the measured MFI-UF (at constant flux) can be used in a model to predict the rate of particulate fouling during RO system operation [4,11].

The MFI-UF test is performed in dead-end filtration mode. Hence, all particles in the feed water move directly towards the surface of the MFI-UF membrane during the test. However, RO plants are typically operated in cross-flow filtration mode, where the particles in the RO feed water either move towards the RO membrane surface or are transported to the concentrate [12]. The portion of particles depositing on RO membranes can be determined by the particle deposition factor proposed by Schippers, et al. [4], by taking in account the difference in particle concentration between the RO feed and RO concentrate. Consequently, the particle deposition factor is incorporated in the MFI-UF model to consider only that portion of particles depositing on RO membranes during cross-flow filtration [4,11].

Sim, et al. [13] and Sim, et al. [14] proposed another approach to simulate particle deposition in RO filtration; i.e. using a cross-flow sampler (CFS) prior to the MFI-UF set-up. The function of the CFS is to fractionate the particles in the feed water under the same hydrodynamic conditions as in RO cross-flow filtration. For this purpose, a non-retentive membrane with large, straight-through pores is used ( $\geq 5 \mu m$ ) in the CFS, so that all particles moving near the membrane surface can permeate through. Subsequently, the permeate collected from the

CFS should contain all potential particles which will likely deposit on the RO membrane. Despite the innovation of this method in simulating RO cross-flow filtration, it does not consider the potential detachment of particles deposited on the RO membrane during actual operation. However, in RO cross-flow filtration, particle deposition is not static and the particles already deposited on the membrane can be re-suspended and transported away from the membrane as a result of the hydrodynamic forces induced on the particles by the tangential flow as well as upon the collision with other flowing particles [5,15]. Accordingly, the MFI-UF method incorporating the concept of a particle deposition factor has the advantage that it can reflect both the deposition of particles as well as the detachment of particles from the RO membrane by considering the actual particle load in both the RO feed and RO concentrate.

Particulate fouling rates predicted based on the MFI-UF can depend strongly on the testing conditions applied during the MFI-UF test, namely; flux rate and UF membrane molecular weight cut-off (MWCO), as explained below.

The measured MFI-UF can be greatly affected by the flux rate applied during the MFI-UF test. At higher flux (i.e. higher permeation rate), the particles in the cake can be re-arranged, and simultaneously the cake can be compressed. As a result, the cake resistance and thus the measured MFI-UF will increase. Hence, the MFI-UF should be typically measured at the same flux rate as is applied in the RO system ( $\sim 10\text{--}35 L/m^2 \cdot h$ ). However, for a fixed feed volume, the filtration time and thus the time required to build a cake/gel on the MFI-UF membrane is significantly longer at lower flux. Therefore, to deal with this problem, Salinas-Rodríguez, et al. [16] proposed to measure the MFI-UF at higher flux rates (e.g.  $50\text{--}350 L/m^2 \cdot h$ ) and extrapolate to the actual flux rate in the RO system. However, the MFI-UF values determined by both approaches (i.e. direct measurement and extrapolation) have not yet been compared, and hence, it is unknown whether both approaches yield similar MFI-UF results.

The MWCO of the MFI-UF membrane can also substantially affect the measured MFI-UF. The lower the membrane MWCO, the smaller the membrane pore size and the more particles can be retained by the MFI-UF membrane, which eventually leads to higher MFI-UF value [11]. In addition, it was found in a previous study [17] that MFI-UF membranes with lower MWCO have lower surface porosity and thus smaller effective filtration area. This results in a higher local flux during the MFI-UF test and subsequently an overestimation of the MFI-UF value. Abunada, et al. [17] quantified the effect of membrane surface porosity on the MFI-UF using a suspension of polystyrene particles. As a result, a correction factor was proposed for the MFI-UF measured with 5–100 kDa membranes by a factor of 0.4–1.0, respectively. Accordingly, there is a need to further investigate the effect of MFI-UF membrane MWCO (i.e. both pore size and surface porosity) on the particulate fouling rate prediction.

This study aims to apply and verify the MFI-UF method to predict the rate of particulate fouling under various MFI-UF testing conditions. For this purpose, the MFI-UF was measured at two full-scale RO plants, using 5–100 kDa UF membranes. The objectives were as follows.

- I. To measure the MFI-UF of RO feed and RO concentrate at the same (low) flux applied in RO plants. The MFI-UF was measured (1) directly at the same low flux applied in the RO plants, and (2) at higher flux rates ( $50\text{--}200 L/m^2 \cdot h$ ) and then the MFI-UF was extrapolated to the same low flux as was applied in the RO plant. Finally, the MFI-UF values measured by both approaches were compared.
- II. To measure the particle deposition factor to account for the fractions of particles depositing during RO cross-flow filtration.
- III. To predict the particulate fouling rate (based on the measured MFI-UF of RO feed and deposition factor), and compare it with the actual fouling rate observed in the RO plants.

## 2. Background: MFI-UF theory

Membrane particulate fouling occurs typically in three subsequent mechanisms; (i) pore blocking, (ii) cake/gel filtration, and (iii) cake/gel compression, as shown in Fig. 1. However, for RO membranes, cake/gel filtration is considered the dominant particulate fouling mechanism (Zhu and Elimelech, 1997). Therefore, the MFI-UF method was derived based on the cake/gel filtration to closely simulate particulate fouling in RO systems, as explained below.

At constant flux (i.e. operation mode of most RO systems), cake/gel filtration can be described by the fundamental model shown in Eq. (1) [10].

$$J = \frac{\Delta P}{\eta \cdot (R_m + R_c)} \quad (1)$$

where  $J$  is the flux,  $\Delta P$  is the transmembrane pressure,  $\eta$  is water viscosity,  $R_m$  is the clean membrane resistance and  $R_c$  is the cake/gel resistance.

At constant flux filtration,  $R_c$  can be described as a function of time, as shown in Eq. (2).

$$R_c = J \cdot I \cdot t \quad (2)$$

The parameter  $I$  is the fouling index, which describes the fouling potential due to cake/gel formed on the membrane surface.

With combining and rearranging Eqs. (1) and (2), cake/gel filtration at constant flux can be then defined by Eq. (3).

$$\Delta P = J \cdot \eta \cdot R_m + J^2 \cdot \eta \cdot I \cdot t \quad (3)$$

Cake/gel filtration in RO can be simulated during MFI-UF test (i.e. by filtering the feed water through UF membrane at constant flux), as shown in Fig. 1.

Subsequently, the value of  $I$  (fouling index) is determined from the slope of the linear cake/gel filtration phase, as shown in Eq. (4).

$$I = \frac{1}{J^2 \cdot \eta} \cdot \text{slope} \quad (4)$$

By definition, the MFI-UF is the  $I$  value corrected to reference testing conditions, as shown in Eq. (5).

$$MFI - UF = \frac{\eta_{20^\circ C} \cdot I}{2 \cdot \Delta P_o \cdot A_o^2} \quad (5)$$

where  $\Delta P_o$ ,  $\eta_{20^\circ C}$  and  $A_o$  are, respectively, the reference pressure (200 kPa), water viscosity ( $1 \times 10^{-6}$  kPa.s) and surface membrane area ( $13.8 \times 10^{-4}$  m<sup>2</sup>) [18].

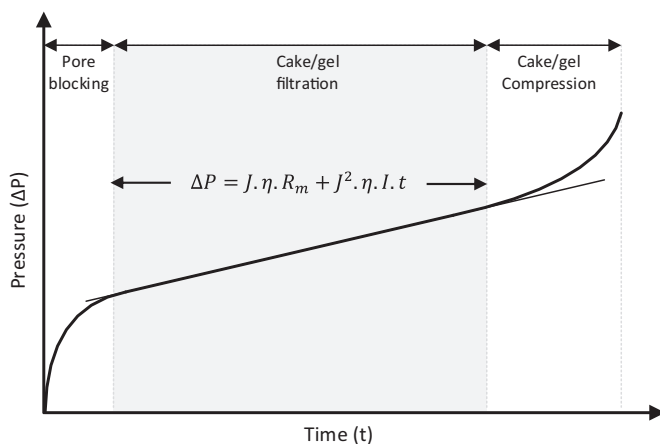


Fig. 1. Typical particulate fouling mechanisms during MFI-UF test performed at constant flux.

### 2.1. MFI-UF fouling prediction model

Particulate fouling development rate at constant flux filtration can be described by the increase of the net driving pressure (NDP) over a certain time, assuming that the NDP increase is mainly attributable to the cake/gel formed by particulate matter with a negligible contribution by scaling and biofouling. Accordingly, the NDP increase ( $\Delta NDP$ ) during a certain period of time ( $t$ ) can be determined by integrating Eq. (3) from  $t = 0$  to  $t = t$ , as shown in Eq. (6), where  $\Delta P_{t=0}$  is an initial NDP pressure value at a reference time and  $\Delta P_{t=t}$  is the NDP pressure value after time ( $t$ ).

$$\Delta NDP = \Delta P_{t=t} - \Delta P_{t=0} = J^2 \cdot \eta \cdot I \cdot t \quad (6)$$

By substituting the value of  $I$  from Eq. (5), the NDP increase rate can be then predicted based on the measured MFI-UF using the model shown in Eq. (7) [4].

$$\frac{\Delta NDP}{t} = \frac{2 \Delta P_o \cdot A_o^2 \cdot J^2 \cdot \eta \cdot \Omega \cdot MFI - UF_{feed}}{\eta_{20^\circ C}} \quad (7)$$

The particle deposition factor ( $\Omega$ ) incorporated in the prediction model (Eq. (7)) simulates the portion of particles depositing on the RO membrane during cross-flow filtration. The deposition factor can be determined by Eq. (8), based on  $R$  (recovery rate; the ratio of RO permeate flow to RO feed flow),  $MFI - UF_{feed}$  (MFI-UF of RO feed) and  $MFI - UF_{concentrate}$  (MFI-UF of RO concentrate). Ideally, the  $\Omega$  has a value between 0 and 1; where,  $\Omega = 0$  indicates no particle deposition, and  $\Omega = 1$  indicates that all particles presented in the feed water passing the RO membrane deposited and remained on its surface [4,11,19].

$$\Omega = \frac{1}{R} + \frac{MFI - UF_{concentrate}}{MFI - UF_{feed}} \cdot \left(1 - \frac{1}{R}\right) \quad (8)$$

## 3. Materials and methods

To achieve the objectives of this study aiming at verifying the MFI-UF method to predict the particulate fouling rate in full-scale RO plants, the main steps shown in Fig. 2 were followed, where the materials/methods applied in each step are explained in detail in the following sub-sections.

### 3.1. Full-scale RO plants and sample collection

#### 3.1.1. RO plant description

The MFI-UF was applied to predict the particulate fouling rate in two different full-scale RO plants treating surface water, located in the

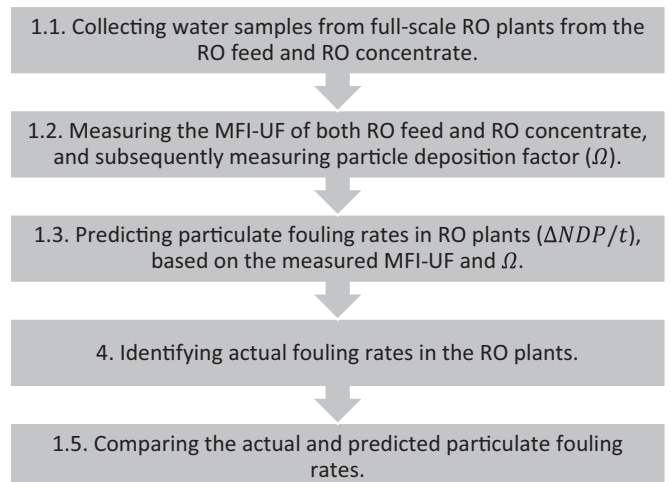


Fig. 2. Methodology followed to verify the MFI-UF method to predict the particulate fouling rate in full-scale RO plants.

Netherlands. The scheme of the main treatment processes of each plant is shown in Fig. 3.

Plant A (Fig. 3 (top)) is a full-scale RO plant, producing drinking water with an average capacity of 2000 m<sup>3</sup>/h. The plant receives raw water from a lake. The raw water is treated first by serial conventional pre-treatment processes, including micro strainers, coagulation/flocculation (using 20 mg/L Fe<sup>3+</sup> as coagulant), sedimentation, and rapid sand filtration (10–20 m/h). The pre-treated water is then transported via 80 km pipeline and filtered through 150 kDa UF membranes (X-flow XIGA 40, Pentair). To prevent the occurrence of scaling, a dose of 1.8 mg/L of antiscalant is injected into the feed water after the UF. Finally, the feed water is pumped into 8 parallel units of 8” RO membranes (ESPA3 24, Hydranautics) with a total recovery of 80 %. All RO units receive same RO feed and operate at same conditions. In addition, all RO units have same configuration consisting of 2 stages (24:12 pressure vessels - 7 RO membrane elements per vessel).

Plant B (Fig. 3 (bottom)) is a full-scale RO plant, producing industrial water with an average capacity of 800 m<sup>3</sup>/h, by treating raw water received from a river. The raw water is first conventionally pre-treated by strainers and combined coagulation (2 mg/L Fe<sup>3+</sup>), dissolved air flotation (DAF) and media filtration. Subsequently, the scaling compounds in the pre-treated water are removed by a softening process (ion exchange) which is followed by NaOH addition to adjust the pH (to pH = 9.3) to prevent the biofouling in the downstream RO units. The water is then prefiltered through cartridge filters (CF) with pore size of 10 μm, and finally pumped to 4 parallel units of 8” RO membranes (FILMTEC ECO PRO-440i, Dupont) with a total recovery of 85 %. All RO units receive same RO feed and operate at same conditions. In addition, all RO units have same configuration consisting of 3 stages (24:12:6 pressure vessels - 6 RO membrane elements per vessel).

The detailed specifications of RO membranes installed in both plants are shown in Appendix A in the supplementary material.

3.1.2. Water samples

Four different sets of water samples were collected from the RO plants as described in Tables 1 and 2. One RO unit was targeted from

**Table 1**  
Summary of water samples collection and operational data.

|         | Trial (#) | Time          | RO stage | Avg. J (L/m <sup>2</sup> .h) | R (%) |
|---------|-----------|---------------|----------|------------------------------|-------|
| Plant A | 1         | January 2019  | Stage 1  | 23                           | 55    |
|         | 2         | January 2021  | Stage 1  | 26                           | 57    |
|         | 3         | March 2021    | Stage 1  | 26                           | 57    |
| Plant B | 1         | December 2019 | Stage 1  | 20                           | 51    |
|         |           |               | Stage 2  | 20                           | 53    |

**Table 2**  
Characteristics of RO feed during collection time.

| Parameter         | Plant A        | Plant B      |
|-------------------|----------------|--------------|
| Cations:          |                |              |
| Calcium           | 57–65 mg/L     | < 3 mg/L     |
| Magnesium         | 11–17 mg/L     | < 0.4 mg/L   |
| Sodium            | 66–122 mg/L    | –            |
| Iron              | < 0.01 mg/L    | < 0.005 mg/L |
| Barium            | 0.03–0.04 mg/L | –            |
| Strontium         | 0.36–0.46 mg/L | –            |
| Anions:           |                |              |
| Carbonate         | < 5 mg/L       | –            |
| Chloride          | 130–220 mg/L   | –            |
| Silicat           | 1.4–4.2 mg/L   | 5 mg/L       |
| Sulphate          | 56–76 mg/L     | 54 mg/L      |
| Bicarbonate       | 148–152 mg/L   | 160 mg/L     |
| Other parameters: |                |              |
| Temperature       | 4–5 °C         | 7 °C         |
| pH                | 7.8–8.0        | 9.3          |
| EC                | 690–980 uS/cm  | 780 uS/cm    |
| TDS               | 450–640 mg/L   | 510 mg/L     |

each plant, as the operation conditions were similar in all the units of each plant (as explained in Section 3.1.1). Water samples were collected from the RO feed and RO concentrate of the first stages only (as shown in Fig. 3) to eliminate as much as possible the potential effect of scaling on the NDP (since membrane scaling usually occurs in the last stage).

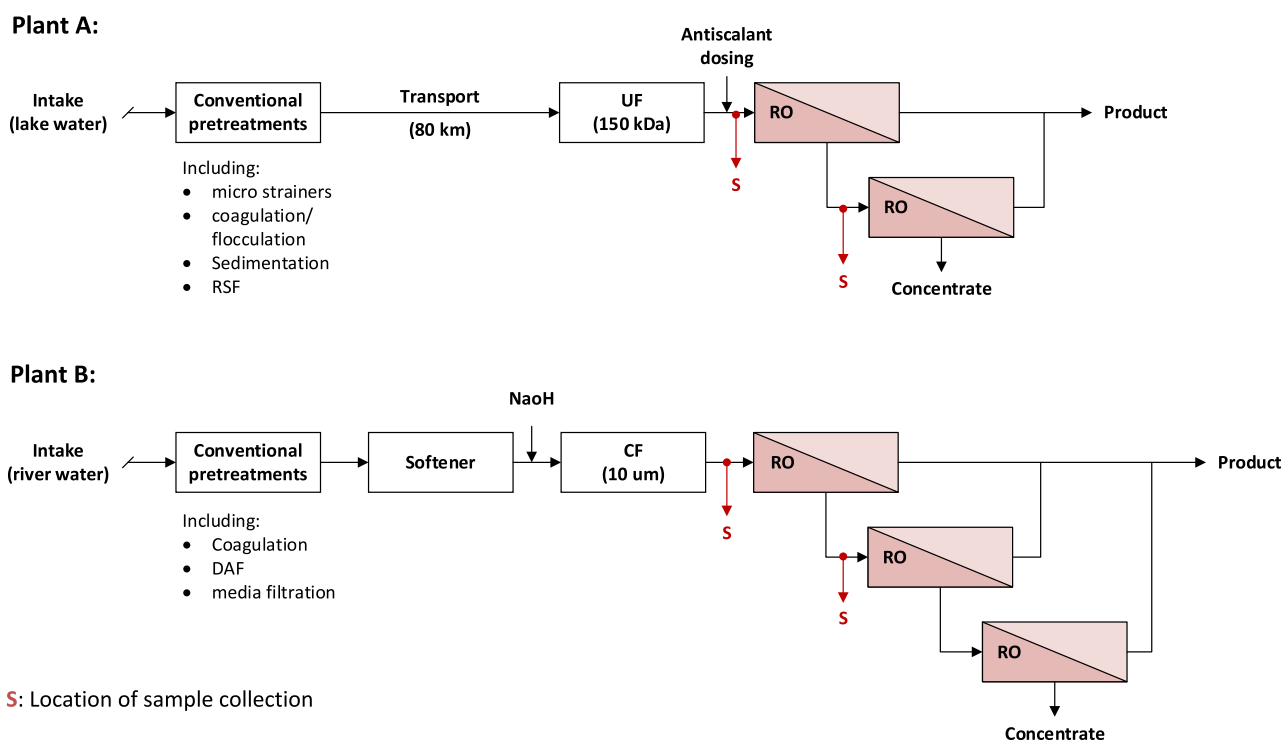


Fig. 3. Treatment process schemes of the studied RO plants.

### 3.2. MFI-UF measurement

#### 3.2.1. MFI-UF set-up

MFI-UF measurements of RO feed and RO concentrate were performed using the set-up schemed in Fig. 4. The set-up consists of three main items: (i) infusion syringe pump (PHD ULTRA, Harvard Apparatus), (ii) pressure transmitter (PXM409, Omega and PMC51, Endress+Hauser), and (iii) membrane holder (Whatman) where the UF membrane is placed. The accuracy of MFI-UF set-up was checked frequently during this study (accuracy check protocol is explained in detail in Appendix B in the supplementary material).

MFI-UF was measured by filtering the feed water through the membrane by pump infusion at constant flow. Pump flow ( $Q$ ) was set based on the membrane surface area ( $A$ ) and the required flux rate ( $J$ ), where  $Q = A \times J$ . The data of the transmembrane pressure ( $\Delta P$ ) development over time ( $t$ ) observed during the MFI-UF test was recorded by the pressure transmitter (every 10 s). Finally, the relationship of  $\Delta P$  against  $t$  was plotted, and then the MFI-UF value was calculated using Eq. (5), as described in Section 2.

#### 3.2.2. MFI-UF membranes

MFI-UF measurements were performed with Polyethersulfone (PES) UF membranes (Millipore) with MWCO of 5, 10, and 100 kDa. The membranes had a flat-sheet configuration and had a diameter of 25 mm. All membranes were cleaned before use to remove the preservation coating. This was done by filtering at least 100 mL of ultra-pure water (Milli-Q®, Millipore) through the membrane at a flux of 200–300 L/m<sup>2</sup>.h. Subsequently, the clean membrane resistance ( $R_m$ ) was measured using Eq. (9).

$$R_m = \frac{\Delta P}{J \cdot \eta} \quad (9)$$

#### 3.2.3. Flux rate

The MFI-UF was measured based on two flux approaches; (1) directly at the same average flux applied in RO plant (20–26 L/m<sup>2</sup>.h), and (2) at higher flux rates (50–200 L/m<sup>2</sup>.h) and then extrapolated to the same average RO flux as proposed by Salinas-Rodríguez, et al. [16]. The outputs of both approaches were compared.

#### 3.2.4. MFI-UF correction for membrane surface porosity effect

In a previous study [17], the effect of surface porosity of MFI-UF membranes was quantified independently of the membrane pore size, using a suspension of washed polystyrene particles. It was found that the lower the membrane surface porosity, the more non-uniformly the membrane pores are distributed, and the smaller the effective membrane filtration area, which subsequently results in a higher local flux rate during the MFI-UF test and eventually leads to an overestimated MFI-UF value. This effect is exacerbated as the MWCO of the MFI-UF

membrane reduces from 100 down to 5 kDa. Accordingly, a correction factor of 0.4 and 0.5 were proposed to correct the MFI-UF measured with 5 and 10 kDa membranes, respectively, while the MFI-UF measured with 100 kDa membrane was not corrected as the effect of membrane surface porosity was expected to be minimal as the pores appeared to be evenly distributed over the membrane surface of the 100 kDa MFI-UF membrane.

Therefore, all MFI-UF values measured with 5 and 10 kDa membranes in this work were corrected to eliminate the effect of membrane surface porosity based on the aforementioned correction factors.

### 3.3. Prediction of particulate fouling rates in RO plants

Particulate fouling rate in the RO plants was predicted using Eq. (7) based on the measured MFI-UF of RO feed and the particle deposition factor (Eq. (8)). The prediction was determined based on the average flux applied in the RO plant (Table 1), at reference temperature condition (25 °C).

### 3.4. Identification of actual fouling observed in RO plants

The actual fouling rate in the RO plants was described by the rate of NDP increase observed over time. However, to verify that the NDP increase is dominated by particulate fouling, the role of the other types of fouling; i.e. scaling, biofouling and organic fouling was also investigated, as follows.

For scaling, the saturation index (SI) of the scaling compounds were determined for the RO concentrate to assess the occurrence of scaling in the RO plants.

Biofouling potential was measured using both bacterial growth potential (BGP) and assimilable organic carbon (AOC) methods. These two methods indicate the potential of bacteria to grow by utilizing biodegradable organic matter present in the sample. BGP was measured as described by Abushaban, et al. [20], where water samples were pasteurized to inactivate microorganisms present in the samples and thereafter distributed in triplicate into 30 mL carbon-free vials and each vial was inoculated with an indigenous microbial consortium from the intake of the RO plant (10,000 intact cells/mL measured by flow cytometry). Bacterial growth was monitored using microbial ATP measurement [21]. The maximum growth was converted to carbon concentration using a calibration line (between glucose and maximum bacterial growth). Whereas AOC was measured following the protocol proposed by Kooij [22] which has similar concept of BGP. However, in AOC test, the samples were incubated by *Pseudomonas fluorescens* P17 and *Spirillum* sp. NOX bacteria and the bacterial growth was monitored by heterotrophic plate counting (HPC). To convert bacterial growth to carbon, acetate is used for AOC test while glucose is used for BGP measurements.

Finally, the organic carbon content of the RO feed was measured as dissolved organic carbon (DOC).

#### 3.4.1. NDP calculation and normalization

The actual fouling in the RO plants was determined by calculating the NDP overtime, using Eq. (10).

$$NDP_{act} = P_f - \frac{dP}{2} - \Delta P_{osm} - P_p \quad (10)$$

where  $P_f$  is the feed pressure,  $P_p$  is the permeate pressure,  $dP$  is the average pressure drop across the RO membrane (feed pressure - concentrate pressure), and  $\Delta P_{osm}$  is the differential osmotic pressure.

However, the actual NDP development observed in RO plant could be attributable not only to membrane fouling but also the variations in operational parameters, namely; (i) permeate flux, and (ii) water temperature (based on Eq. (3)). For this reason, the NDP had to be normalized based on a reference flux and temperature to ensure that the

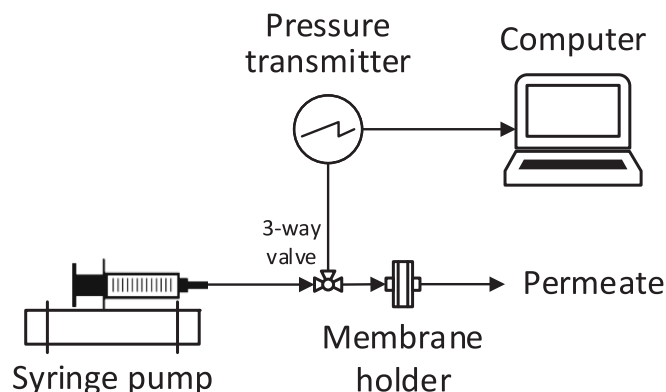


Fig. 4. Scheme of MFI-UF set-up at constant flux filtration.

NDP increase in the plant is only due to membrane fouling and not to changes in flux rate and/or water temperature. Accordingly, the NDP was normalized based on Eqs. (11)–(13).

$$NDP_{nor} = NDP_{act} \frac{FCF}{TCF} \tag{11}$$

$$FCF = \frac{J_r}{J_a} \tag{12}$$

$$TCF = e^{3020 \left( \left( \frac{1}{T_a + 273} \right) - \left( \frac{1}{T_r + 273} \right) \right)} \tag{13}$$

where:

*FCF* is the flux correction factor. It corrects the NDP for the flux linearly (since the NDP is linearly correlated to the flux based on Eq. (1)).

*TCF* is the temperature correction factor.

*J<sub>r</sub>* is the reference flux. It was substituted by the average flux in the RO plant during the fouling prediction period (Table 1).

*J<sub>a</sub>* is the actual flux.

*T<sub>r</sub>* is the reference water temperature at standard condition (25 °C).

*T<sub>a</sub>* is the actual water temperature.

### 3.5. Comparison between predicted and observed fouling rates in RO plants

Finally, the fouling rates (i.e. NDP increase rates) predicted based on MFI-UF prediction model (Eq. (7)) were plotted together with the normalized NDP increase observed in the RO plants, to verify the accuracy of MFI-UF method. The comparison between the predicted and observed fouling rates was based on the assumption that no variation in the quality of RO feed occurs after sample collection. Nevertheless, as this might not be the case in reality, the comparison between the predicted and observed fouling rates was limited to 30 days after sample collection, assuming minor variation in the quality of RO feed water may occur during this period. However, for plant B, the fouling rates were predicted only over 7 days, since the RO membranes in the plant were cleaned on weakly basis (due to the high pressure drop observed in the plant) during the time of this work.

## 4. Results and discussion

### 4.1. MFI-UF of RO feed and RO concentrate

Fig. 5 shows the MFI-UF of RO feed and RO concentrate of stage 1 in plant A (Trial #1) using 5, 10 and 100 kDa membranes. The MFI-UF was

measured based on two flux approaches; (1) directly at the same average RO flux applied in the plant which was 23 L/m<sup>2</sup>.h (open points), and (2) at higher flux rates; 50, 100 and 200 L/m<sup>2</sup>.h (solid points) and then extrapolated linearly at the average RO flux in the plant (disconnected lines). As can be observed in all cases, the MFI-UF values measured at 23 L/m<sup>2</sup>.h and those extrapolated were very similar, with a difference of around ±5 % (detailed MFI-UF values are in Appendix C in the supplementary material). Hence, the results indeed confirmed that even at low flux rates the MFI-UF can be measured directly or extrapolated from the MFI-UF values measured at higher flux rates, as both approaches eventually yield similar output.

Accordingly, the MFI-UF was measured in the two RO plants selected for this study based on both approaches (the results are presented in Appendix C in the supplementary material). The MFI-UF measurement based on the second approach (i.e. extrapolation from higher flux rates) was also investigated based on other flux ranges; where the MFI-UF was extrapolated based on only 2 flux rate experiments (100 and 200 L/m<sup>2</sup>.h) as well as with 3 flux rate experiments with equal increment (100, 150 and 200 L/m<sup>2</sup>.h). The results showed that the MFI-UF extrapolated based on the 3 flux rate experiments appeared more accurate. This is because in the case of 2 flux rate experiments, the regression line is defined by only 2 data points, and therefore, any uncertainty in the MFI-UF measured at the higher flux rates (i.e. 100 and 200 L/m<sup>2</sup>.h) will impact the MFI-UF value extrapolated at the low RO flux. In addition, the results showed that measuring the MFI-UF at higher flux rates with equal-increments (i.e. 100, 150 and 200 L/m<sup>2</sup>.h) could eliminate the potential influence of high leverage on the resulted regression line and thus on the extrapolated MFI-UF value.

The linear correlation between the MFI-UF and flux rate found in this study agree with the observation of Salinas-Rodríguez, et al. [16] who also found a linear correlation for various types of feed water. However, the relationship of the MFI-UF and flux rate may not be ultimately linear for all types of feed water. This is because the rate of cake compressibility due to the increasing flux may not be constant (as the case in this sturdy) and it may vary depending on the characteristics of particles existing in the feed water.

#### 4.1.1. Dependency of MFI-UF test duration on the applied flux

Table 3 shows the duration range of the MFI-UF measurements discussed above in relation to the flux rate applied during the MFI-UF test. As it can be clearly observed, the duration of the MFI-UF measurement performed based on flux approach (1) was substantially longer than that performed based on approach (2). The reason is because the lower the flux, the lower the load of particles depositing on the membrane. Consequently, the depositing particles take longer time to interconnect and build-up a complete cake in even layers on the membrane surface

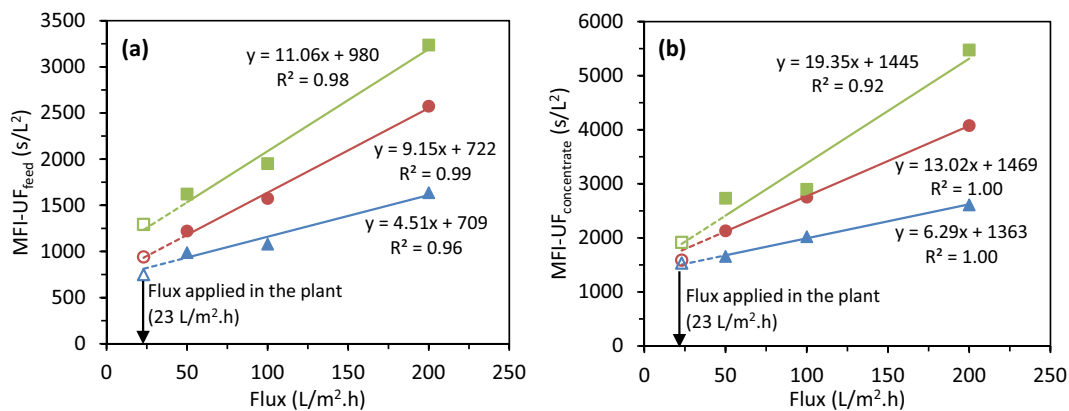


Fig. 5. MFI-UF measured in plant A – stage 1 (Trial #1): (a) RO feed, and (b) RO concentrate; (i) MFI-UF measured directly at same RO flux applied in the plant (△ 100 kDa, ○ 10 kDa, □ 5 kDa), and (ii) MFI-UF measured at higher flux rates (▲ 100 kDa, ● 10 kDa, ■ 5 kDa) and extrapolated at the applied RO flux (disconnected lines).

**Table 3**  
Approximate duration of MFI-UF test performed based on the applied flux rate.

|   | Flux                      | MFI-UF test duration |
|---|---------------------------|----------------------|
| Approach (1): MFI-UF measured directly at the same flux applied in the RO plant                                   | 20–26 L/m <sup>2</sup> .h | 500–800 min          |
| Approach (2): MFI-UF measured at higher flux rates and then extrapolated at the same flux applied in the RO plant | 50 L/m <sup>2</sup> .h    | 90–120 min           |
|   | 100 L/m <sup>2</sup> .h   | 60–90 min            |
|   | 150 L/m <sup>2</sup> .h   | 60–70 min            |
|   | 200 L/m <sup>2</sup> .h   | 30–60 min            |

[17].

In addition, in this work, the overall time of the MFI-UF measurements performed based on approach (2) was much faster than in the case of approach (1). However, approach (2) had one disadvantage in that it requires more effort since multiple MFI-UF measurements should be performed to determine the MFI-UF at the actual RO flux, while only one MFI-UF measurement is required in case approach (1) is applied. Accordingly, the best approach can be selected by trading off the time against the cost and effort.

It is important to mention that the duration of MFI-UF tests listed in Table 3 depended mainly on the characteristics of feed water measured in this study. Therefore, different duration might be required for other types of feed water even if the MFI-UF is measured at the same testing conditions (i.e. same MFI-UF membrane and flux rate).

#### 4.1.2. Particle deposition factor

Table 4 shows the particle deposition factors ( $\Omega$ ) in the full-scale RO plants. In general, higher particle deposition factor ( $\Omega$ ) was found when the MFI-UF was measured using lower MWCO UF membrane (for plant A - Trial #2, the difference in the  $\Omega$  was minor). Exceptionally, in plant A (Trail #3), the particle deposition factor ( $\Omega$ ) measured based on the 5 kDa membrane was negative. The negative  $\Omega$  value indicates that the load of particles detached from the RO membrane was higher than that of particles depositing on the membrane [5]. However, since the  $\Omega$  values measured based on both 10 and 100 kDa membranes were positive, this could indicate that particle detachment occurred only for particles smaller than 10 kDa. This could be explained by the effect of cross-flow hydrodynamic conditions on the cake stratification, which could result in smaller particles concentrating on the top of the cake and larger particles in the bottom [23]. As a result, the smaller particles might detach from the top of the cake by the hydrodynamic forces induced on the particles by the tangential flow as well as due to the collision with other flowing particles [15]. The reason that particle detachment occurred only in this Trail (i.e. not in Trial #1 nor 2) might be because the thickness of the cake accumulated on the RO membranes was higher during the time of this Trial, and thus the chance of particle detachment due to the acting tangential forces was higher [5].

Interestingly, for plant B, particle deposition factor ( $\Omega$ ) in stage 1 were higher than the corresponding values for stage 2, although both stages operated at similar flux and cross-flow velocity. This could be because the concentration (i.e. load) of particles in the feed of stage 2

**Table 4**  
Particle deposition factor ( $\Omega$ ) measured at the same flux applied in RO plant.

|         | Trial (#) | RO stage | $\Omega$ values |        |       |
|---------|-----------|----------|-----------------|--------|-------|
|         |           |          | 100 kDa         | 10 kDa | 5 kDa |
| Plant A | 1         | Stage 1  | 0.12            | 0.44   | 0.61  |
|         | 2         | Stage 1  | 0.57            | 0.59   | 0.62  |
|         | 3         | Stage 1  | 0.70            | 0.81   | -0.72 |
| Plant B | 1         | Stage 1  | 0.67            | 0.89   | 0.90  |
|         |           | Stage 2  | 0.38            | 0.42   | 0.60  |

was higher, as indicated from the MFI-UF values. Hence, there was a higher chance of collision between the particles moving by the tangential flow across the RO membranes and the particles which already deposited. Consequently, this collision might have reduced the particle deposition on RO membrane, which eventually resulted in lower  $\Omega$  values. However, this hypothesis/explanation still needs further investigation.

#### 4.2. Actual fouling observed in the RO plants

Figs. 6 and 7 show the actual fouling observed in plant A and B, respectively, expressed in NDP increase overtime. In principle, the NDP increase can be due to scaling, biological fouling, organic fouling and/or particulate fouling or a combination of all these fouling phenomena. However, the NDP increase in the RO plants was assumed to be mainly due to particulate fouling (i.e. formation of cake/gel by particles/colloids accumulated on the RO membrane surface), as indicated by the measured fouling indices/parameters shown in Table 5 and explained below.

##### 4.2.1. Plant A

For plant A, scaling is controlled by dosing antiscalant to the RO feed (1.8 mg/L). In the RO concentrate, calcium carbonate and barium sulphate were slightly supersaturated (SI = 0.7–1.0 and 1.9–2.8, respectively) and their saturation level was in the range which can be controlled by the antiscalant [24,25].

Biofouling is not expected to be the reason for the NDP increase in plant A, since the measured AOC concentration in the RO feed is very low (3–6  $\mu\text{g/L}$ ). Vrouwenvelder and van der Kooij [26] observed RO biofouling when AOC concentration in the feed water exceeded 80  $\mu\text{g/L}$ . Moreover, Weinrich, et al. [27] reported that bacterial growth in the absence of a chlorine residual can be observed at AOC concentration of 10  $\mu\text{g/L}$  or higher.

Organic fouling due to the adsorption of dissolved organic matter onto the surface of RO membranes was not expected to be a problem in plant A, as organic fouling is assumed to occur prior to cake/gel formation when new/clean membranes are put into operation. However, the RO membranes of plant A was already in operation for around 6 months and any adsorption onto the RO membrane would have already taken place. The negligible effect of organic fouling (and also biofouling) can be supported by the normalized pressure drop ( $dP$ ) observed across stage 1, which was stable (i.e. not increasing) during the fouling prediction period (pressure drop data is shown in Appendix D in the supplementary material). It is important to mention that the stable pressure drop does not rule out the particulate fouling in the plant, since the particles/colloids existed in the RO feed (pretreated by 150 kDa UF) might have passed through the feed spacers in the RO membranes (i.e. did not cause any increase in the pressure drop) but deposited and accumulated on the surface of the membranes resulting in NDP increase.

According to the above explanation, it could be concluded that particulate fouling is most likely the main reason for the NDP increase in Plant A. The existence of particulate matter (i.e. particles/colloids) in the RO feed after the extensive pre-treatment enhanced by UF, could be a result of several reasons; (i) the passage of small colloids through the UF, (ii) loss of integrity of the UF which could allow to the larger particles/colloids to pass into the permeate side (i.e. RO feed), (iii) re-aggregation of small particles/colloids that passed through the UF, and/or (iv) re-growth of bacteria on the permeate side of the UF membranes (which are considered as particles).

##### 4.2.2. Plant B

In plant B, the concentrations of sparingly soluble compounds were reduced substantially prior to the RO units by the softening process (as shown in Table 2). Therefore, the scaling compounds were undersaturated in the RO concentrate, and hence scaling was not expected to occur in the plant.



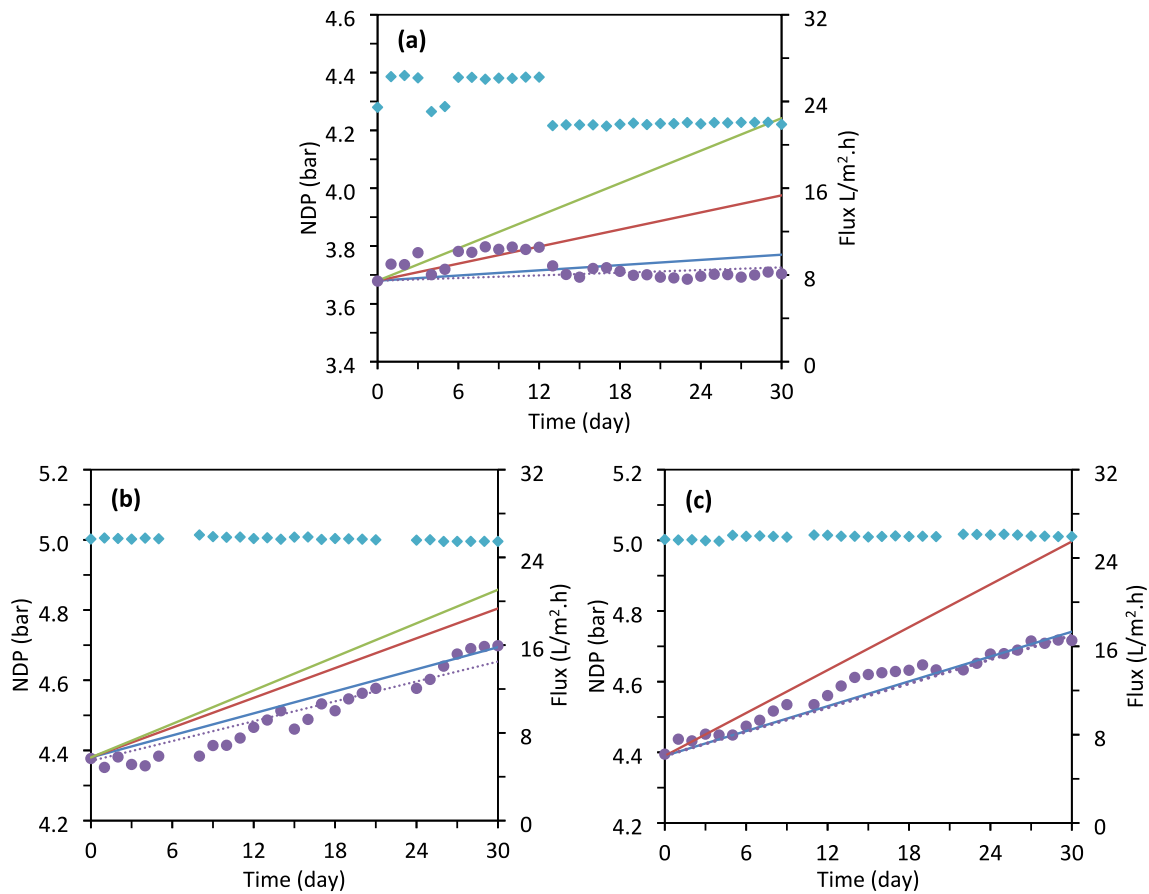


**Fig. 6.** Predicted and observed NDP increase along with the flux applied in plant A – stage 1 (where day 0 is the day of sample collection) (a) Trial #1, (b) Trial #2, and (c) Trial #3  
 Predicted NDP - MFI-UF<sub>100</sub> kDa (—), predicted NDP - MFI-UF<sub>10</sub> kDa (—), predicted NDP - MFI-UF<sub>5</sub> kDa (---), observed NDP (●), observed NDP trend (---), and flux (◆).

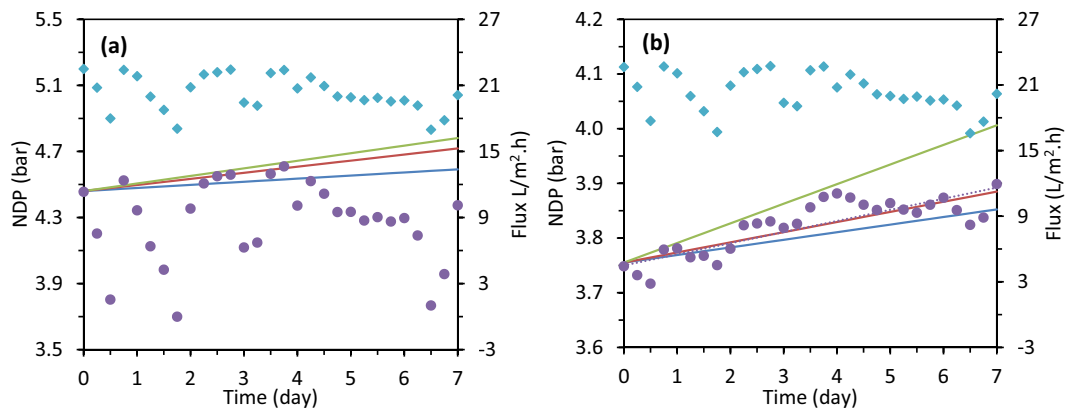


**Fig. 7.** Predicted and observed NDP increase along with the flux applied in plant B (where day 0 is the day of sample collection) (a) stage 1, and (b) stage 2  
 Predicted NDP - MFI-UF<sub>100</sub> kDa (—), predicted NDP - MFI-UF<sub>10</sub> kDa (—), predicted NDP - MFI-UF<sub>5</sub> kDa (---), observed NDP (●), observed NDP trend (---), and flux (◆).

Biofouling is also not expected to be the reason behind the NDP increase in plant B since the pH of the RO feed is adjusted to 9.3 (by adding NaOH) after softening process, in which most bacteria cannot grow or even survive. Moreover, when the pH is corrected to around 8, low BGP concentrations were measured (< 78 µg/L). Abushaban, et al. [28] reported a BGP concentration of 70 µg/L in SWRO feedwater, where the CIP (cleaning in place) is performed every 3 years. Furthermore, the measured orthophosphate concentration in the RO feed (< 0.3 µg/L) is also below the indicated threshold value [29,30].

However, the RO membranes in plant B were cleaned almost every week due to the high pressure drop observed in the plant (around 2.8 bar per stage, normalized based on the worst-case conditions; maximum flow and minimum temperature). The increase in the pressure drop could be due to organic and/or particulate fouling (whereas biofouling effect is considered minor as explained above). Nevertheless, the concentration of DOC in the RO feed was low (1.2–1.5 mg/L), which might indicate less effect due to organic fouling.

Therefore, it could be concluded that particulate fouling is most

**Table 5**  
Measured scaling, biological and organic fouling potential indices/parameters for plant A and B.

| Index/parameter        | Plant A      | Plant B      |
|------------------------|--------------|--------------|
| Scaling:               |              |              |
| SI – CaCO <sub>3</sub> | 0.7–1.0      | –            |
| SI – BaSO <sub>4</sub> | 1.9–2.8      | –            |
| Biofouling potential:  |              |              |
| AOC                    | 3–6 µg/L     | –            |
| BGB                    | –            | 55–78 µg/L   |
| Orthophosphate         | –            | < 0.3 µg-C/L |
| Organic fouling:       |              |              |
| DOC                    | 2.6–3.6 mg/L | 1.2–1.5 mg/L |

likely the dominant type of fouling in plant B, while the effect of organic fouling could not be excluded completely.

#### 4.3. Comparison between predicted and observed fouling rates in RO plants

The comparison between the observed and predicted NDP development (i.e. fouling rate) is presented in Figs. 6 and 7 for plant A and plant B, respectively. As mentioned in Section 3.5, for plant A, the prediction of NDP increase was limited to 30 days, assuming minor variation in the quality of RO feed water may occur during this period. For plant B, the fouling rates were predicted over only 7 days, since the RO membranes in the plant were cleaned almost every week (due to the high pressure drop observed in the plant).

For plant A – Trial #1 (Fig. 6 (a)), the observed NDP was apparently affected by the flux variation in the plant, particularly in the earlier phase (i.e. 0–13 days), although the observed NDP was already normalized for the flux (Section 3.4.1). This is because the flux normalization could correct only the hydrodynamic effect of the flux on the NDP, but it does not take into account the effect of flux on cake compression (i.e. cake resistance). Consequently, the observed NDP rapidly increased on day 1 and 6 due to the cake compression resulting from the flux increase (from 23 to 26 L/m<sup>2</sup>.h), while it suddenly declined on day 4 and 13 as the cake relaxed when the flux decreased again (from 26 to 23 L/m<sup>2</sup>.h). Accordingly, once the flux applied in the plant became constant at 23 L/m<sup>2</sup>.h (day 13–30), the observed NDP development was stable. During this phase, the NDP predicted based on the MFI-UF measured using the 100 kDa membrane showed the best agreement with the observed NDP trend, where the deviation between the predicted and actual fouling rate was around 10 % (Table 6).

In the other trials with plant A (Fig. 6 (b) and (c)), the observed NDP trend was similar. The sudden NDP decline observed during the prediction period was due to turning the RO unit off as some maintenance

**Table 6**  
Summary of the MFI-UF-based predicted NDP increase rates and the average NDP increase trend observed in the RO plants.

|                     | Predicted NDP increase rate (bar/month)                 |                      |                      |
|---------------------|---|----------------------|----------------------|
|                     | [Deviation between observed and predicted NDP increase] |                      |                      |
|                     | 100 kDa   | 10 kDa               | 5 kDa                |
| Plant A: Fig. 6 (a) | 0.06<br>[11 %]  | 0.30<br>[100 %]      | 0.56<br>[>100 %]     |
| Plant A: Fig. 6 (b) | 0.31<br>[8 %]   | 0.42<br>[29 %]       | 0.48<br>[37 %]       |
| Plant A: Fig. 6 (c) | 0.35<br>[3 %]   | 0.60<br>[36 %]       | <sup>a</sup>         |
| Plant B: Fig. 7 (a) | 0.56<br><sup>b</sup>                                    | 1.06<br><sup>b</sup> | 1.46<br><sup>b</sup> |
| Plant B: Fig. 7 (b) | 0.45<br>[15 %]  | 0.56<br>[2 %]        | 1.08<br>[43 %]       |

<sup>a</sup> The NDP was not predicted since the  $\Omega$  had a negative value.

<sup>b</sup> The observed NDP increase could not be identified as the NDP trend was highly unstable.

work were carried out. However, no membrane flushing nor CIP took place during the shut-down period (based on the information obtained from the plant operator). Hence, the NDP dropped probably as a result of cake relaxation due to switching the RO unit off. Nevertheless, the NDP drop was minor (< 0.05 bar). In both trials (Fig. 6 (b) and (c)), the rate of in NDP increase predicted based on the MFI-UF measured with the 100 kDa membrane showed good agreement with the NDP observed in the plant with a deviation of 8 % and 3 % for Trial #2 and #3, respectively (Table 6).

For plant B – stage 1 (Fig. 7 (a)), the observed NDP was significantly affected by the unsteady daily operation of the plant, where it was even difficult to determine the NDP development over time. This was attributed, as mentioned above, to the variation in cake compression resulting from the variable flux applied in the plant. Accordingly, it was not possible to verify the NDP increase rate prediction for stage 1. For stage 2 (Fig. 7 (b)), the effect of the variation in the applied flux on the observed NDP was lower in comparison with stage 1. The reason might be due to the lower load of particles deposited on the RO membranes in stage 2 (Table 4), which resulted in a thinner cake layer on RO membranes. Hence, the variation in the applied flux might have less effect on cake compression. In this case, the NDP increase rate predicted based on the MFI-UF measured with 10 kDa membrane agreed closely with the NDP trend observed in the plant with 2 % deviation (Table 6). The rate of increase in NDP predicted based on the 100 kDa membrane showed also good agreement with the observed NDP with a deviation of 15 % (Table 6).

However, it was expected that fouling prediction would more closely match the actual values when the MWCO of the MFI-UF membrane was lower, since more smaller particles can be captured and evaluated. Nevertheless, this was not the case in the results discussed above; where the fouling rates predicted based on the MFI-UF measured with the 10 and 5 kDa membranes in plant A and the 5 kDa membrane in plant B overestimated the increase in NDP observed over time (by around 30–100 %). This could be attributed to the effect of the non-uniform surface porosity of the MFI-UF membrane, as explained by Abunada, et al. [17]. Although the MFI-UF values were already corrected for the effect of surface porosity (as explained in Section 3.2.4), the correction factors might be still overestimated as these factors were identified based on polystyrene particles which are hardly compressible and are well-defined in size and shape. On the other hand, the real particles present in RO feed water are most likely more compressible and flexible, and they comprise a wide particle size range so that small particles could fill the voids in the formed cake [6,8]. Consequently, the cake formed by particles present in real water (i.e. RO feed) may be more compressed and less porous than a cake formed by polystyrene particles. Therefore, the effect of membrane surface porosity on the cake and thus on the measured MFI-UF may be greater for RO feed water in comparison with a polystyrene particle suspension. As a result, as discussed above, the fouling rates predicted based on the 5–10 kDa membranes were mostly overestimated. In addition, the results also indicated that the correction of MFI-UF for membrane surface porosity effect was dependent on the type of RO feed, where the fouling rate predicted based on 10 kDa membrane was overestimated for plant A but not for plant B, which requires more investigations in the future research.

On the other hand, interestingly, the fouling rates predicted based on the 100 kDa membrane (i.e. the highest MWCO membrane) showed in all cases fairly good agreement with the actual fouling development observed in the RO plant. This could be because the difference in the particle retention by 5, 10 and 100 kDa membranes is small as indicated by the particle deposition factors (Table 4), while the higher fouling rates predicted based on the MFI-UF measured with the 5 and 10 kDa membranes was dominated mainly by the effect of surface porosity as explained above. This could be supported by the scanning electron microscope (SEM) analysis presented by Abunada, et al. [17] which showed that 60–80 % of the pores of the 5–100 kDa membranes had similar size range (6–12 nm), and thus similar particles retention might

be expected with the 5–100 kDa membranes. Furthermore, Boerlage, et al. [31] found that similar retention of particles could be obtained with different MWCO membranes since the cake built-up on the membrane surface could eventually act as a new membrane layer and dominate the filtration, while the role of membrane pore size becomes less dominant over time.

## 5. Conclusions

The MFI-UF method was applied in two full-scale RO plants to predict particulate fouling rate (described by the NDP increase rate). MFI-UF was measured at same flux rates applied in the plants (20–26 L/m<sup>2</sup>.h) using 5–100 kDa membranes. The following are the main findings:

- For plant A, the particulate fouling rates predicted based on the MFI-UF measured with the 100 kDa membranes had the best agreement with the fouling rates observed in the plant with a deviation of 3–11 %.
- For plant B, the particulate fouling rate predicted based on the 10 kDa membrane agreed the best with the fouling observed in the plant with only 2 % deviation. Nevertheless, the fouling rate predicted based on the 100 kDa membrane showed also a good agreement with the observed fouling rate with 15 % deviation.
- Particulate fouling rates predicted based on 5 kDa membrane were considerably overestimated in both RO plants. The reason could be attributed to the effect of surface porosity of 5 kDa membrane, although the MFI-UF values were corrected for this effect. This is because the factors used to correct the MFI-UF for the effect of membrane surface porosity were identified using a suspension of synthetic polystyrene particles [17] which have properties different than those of natural particles in the RO feed.

Accordingly, the findings of this study indicated that the 10–100 kDa is the suitable range of MFI-UF membranes to predict particulate fouling in RO plants. Nevertheless, it is recommended to apply the MFI-UF method in more RO plants operating with different feed water and different conditions, and eventually demonstrate the most suitable range of UF membranes to be used in the MFI-UF measurement for accurate particulate fouling prediction.

In addition, since the accuracy of particulate fouling prediction could be affected by the variation in flux rate and/or feed water quality in RO plants over time, it is recommended to perform the MFI-UF measurement online (i.e. in real-time) over shorter periods (e.g. on monthly basis such as in plant A, or shorter in case the variation is high such as in plant B). Therefore, further research is required to develop a new online and automated MFI-UF measurement system.

## CRedit authorship contribution statement

**Mohanad Abunada:** Conceptualization, Methodology, Validation, Formal analysis, Investigation, Writing – original draft, Visualization, Project administration. **Nirajan Dhakal:** Conceptualization, Methodology, Writing – review & editing, Supervision. **Raffay Gulrez:** Investigation. **Pamela Ajok:** Investigation. **Yuke Li:** Investigation. **Almotasembellah Abushaban:** Conceptualization, Methodology, Investigation, Writing – original draft. **Herman Smit:** Resources. **David Moed:** Resources. **Noreddine Ghaffour:** Conceptualization, Writing – review & editing. **Jan C. Schippers:** Conceptualization, Methodology, Writing – review & editing. **Maria D. Kennedy:** Conceptualization, Methodology, Writing – review & editing, Supervision.

## Declaration of competing interest

The authors declare that they have no known competing financial interests or personal relationships that could have appeared to influence the work reported in this paper.

## Data availability

Data will be made available on request.

## Acknowledgements

The authors would like to gratefully acknowledge PWN and EVIDES water treatment companies in the Netherlands for their cooperation and facilitation to collect samples and operation data from their RO plants. The authors would like also to thank Emmanuelle Prest for providing the AOC data of PWN plant, Vincent Toussaint for providing the operational data of Evides plant, and Nasser Mangal for his support in SI calculation.

## Supplementary data

Supplementary data to this article can be found online at <https://doi.org/10.1016/j.desal.2023.116478>.

## References

- [1] DesalData, IDA Desalination Plants Inventory, 2020.
- [2] ASTM, ASTM D4189-07, Standard Test Method for Silt Density Index (SDI) of Water, West Conshohocken, PA, USA, 2014.
- [3] ASTM, ASTM D8002-15, Standard Test Method for Modified Fouling Index (MFI-0.45) of Water, West Conshohocken, PA, USA, 2015.
- [4] J.C. Schippers, J.H. Hanemaayer, C.A. Smolders, A. Kostense, Predicting flux decline of reverse osmosis membranes, *Desalination* 38 (1981) 339–348, [https://doi.org/10.1016/S0011-9164\(00\)86078-6](https://doi.org/10.1016/S0011-9164(00)86078-6).
- [5] S.F.E. Boerlage, M. Kennedy, M.P. Aniyé, J.C. Schippers, Applications of the MFI-UF to measure and predict particulate fouling in RO systems, *J. Membr. Sci.* 220 (1–2) (2003) 97–116, [https://doi.org/10.1016/S0376-7388\(03\)00222-9](https://doi.org/10.1016/S0376-7388(03)00222-9).
- [6] S.F.E. Boerlage, M.D. Kennedy, M.P. Aniyé, E. Abogrean, Z.S. Tarawneh, J. C. Schippers, The MFI-UF as a water quality test and monitor, *J. Membr. Sci.* 211 (2) (2003) 271–289, [https://doi.org/10.1016/S0376-7388\(02\)00427-1](https://doi.org/10.1016/S0376-7388(02)00427-1).
- [7] S.F.E. Boerlage, M.D. Kennedy, M.P. Aniyé, E.M. Abogrean, D.E.Y. El-Hodali, Z. S. Tarawneh, J.C. Schippers, Modified fouling index ultrafiltration to compare pretreatment processes of reverse osmosis feedwater, *Desalination* 131 (1) (2000) 201–214, [https://doi.org/10.1016/S0011-9164\(00\)90019-5](https://doi.org/10.1016/S0011-9164(00)90019-5).
- [8] S.F.E. Boerlage, M.D. Kennedy, M.P. Aniyé, E.M. Abogrean, G. Galjaard, J. C. Schippers, Monitoring particulate fouling in membrane systems, *Desalination* 118 (1) (1998) 131–142, [https://doi.org/10.1016/S0011-9164\(98\)00107-6](https://doi.org/10.1016/S0011-9164(98)00107-6).
- [9] S.F.E. Boerlage, M.D. Kennedy, P.A.C. Bonne, G. Galjaard, J.C. Schippers, Prediction of flux decline in membrane systems due to particulate fouling, *Desalination* 113 (2) (1997) 231–233, [https://doi.org/10.1016/S0011-9164\(97\)00134-3](https://doi.org/10.1016/S0011-9164(97)00134-3).
- [10] S.F.E. Boerlage, M. Kennedy, Z. Tarawneh, R. De Faber, J.C. Schippers, Development of the MFI-UF in constant flux filtration, *Desalination* 161 (2) (2004) 103–113, [https://doi.org/10.1016/S0011-9164\(04\)90046-X](https://doi.org/10.1016/S0011-9164(04)90046-X).
- [11] S.G. Salinas-Rodríguez, G.L. Amy, J.C. Schippers, M.D. Kennedy, The modified fouling index ultrafiltration constant flux for assessing particulate/colloidal fouling of RO systems, *Desalination* 365 (2015) 79–91, <https://doi.org/10.1016/j.desal.2015.02.018>.
- [12] C.Y. Tang, T.H. Chong, A.G. Fane, Colloidal interactions and fouling of NF and RO membranes: a review, *Adv. Colloid Interf. Sci.* 164 (1–2) (2011) 126–143, <https://doi.org/10.1016/j.cis.2010.10.007>.
- [13] L.N. Sim, Y. Ye, V. Chen, A.G. Fane, Crossflow sampler modified fouling index ultrafiltration (CFS-MFIUF)—an alternative fouling index, *J. Membr. Sci.* 360 (1–2) (2010) 174–184, <https://doi.org/10.1016/j.memsci.2010.05.010>.
- [14] L.N. Sim, Y. Ye, V. Chen, A.G. Fane, Comparison of MFI-UF constant pressure, MFI-UF constant flux and crossflow sampler-modified fouling index ultrafiltration (CFS-MFIUF), *Water Res.* 45 (4) (2011) 1639–1650, <https://doi.org/10.1016/j.watres.2010.12.001>.
- [15] C. Henry, J.-P. Minier, G. Lefèvre, Towards a description of particulate fouling: from single particle deposition to clogging, *Adv. Colloid Interf. Sci.* 185–186 (2012) 34–76, <https://doi.org/10.1016/j.cis.2012.10.001>.
- [16] S.G. Salinas-Rodríguez, M.D. Kennedy, G.L. Amy, J.C. Schippers, Flux dependency of particulate/colloidal fouling in seawater reverse osmosis systems, *Desalin. Water Treat.* 42 (1–3) (2012) 155–162, <https://doi.org/10.1080/19443994.2012.683104>.
- [17] M. Abunada, N. Dhakal, W.Z. Andyar, P. Ajok, H. Smit, N. Ghaffour, J.C. Schippers, M.D. Kennedy, Improving MFI-UF constant flux to more accurately predict particulate fouling in RO systems: quantifying the effect of membrane surface porosity, *J. Membr. Sci.* 660 (2022), 120854, <https://doi.org/10.1016/j.memsci.2022.120854>.
- [18] J.C. Schippers, J. Verdouw, The modified fouling index, a method of determining the fouling characteristics of water, *Desalination* 32 (1980) 137–148, [https://doi.org/10.1016/S0011-9164\(00\)86014-2](https://doi.org/10.1016/S0011-9164(00)86014-2).
- [19] S.G. Salinas-Rodríguez, Particulate and Organic Matter Fouling of Seawater Reverse Osmosis Systems: Characterization, Modelling and Applications, 1st Edition, CRC Press/Balkema, London, UK, 2011.

- [20] A. Abushaban, M.N. Mangal, S.G. Salinas-Rodriguez, C. Nnebuo, S. Mondal, S. Goueli, J. Schippers, M. Kennedy, Direct measurement of ATP in seawater and application of ATP to monitor bacterial growth potential in SWRO pre-treatment systems, *Desalin. Water Treat.* 99 (2017), <https://doi.org/10.5004/dwt.2017.21783>.
- [21] A. Abushaban, Assessing Bacterial Growth Potential in Seawater Reverse Osmosis Pretreatment: Method Development and Applications, 2019, <https://doi.org/10.1201/9781003021940>.
- [22] D.V.D. Kooij, Assimilable organic carbon as an indicator of bacterial regrowth, *J. AWWA* 84 (2) (1992) 57–65, <https://doi.org/10.1002/j.1551-8833.1992.tb07305.x>.
- [23] S.H. Yoon, *Membrane Bioreactor Processes: Principles and Applications*, CRC Press, 2015.
- [24] S.F.E. Boerlage, M.D. Kennedy, I. Bremere, G.J. Witkamp, J.P. Van der Hoek, J. C. Schippers, The scaling potential of barium sulphate in reverse osmosis systems, *J. Membr. Sci.* 197 (1) (2002) 251–268, [https://doi.org/10.1016/S0376-7388\(01\)00654-8](https://doi.org/10.1016/S0376-7388(01)00654-8).
- [25] M.N. Mangal, V.A. Yangali-Quintanilla, S.G. Salinas-Rodriguez, J. Dusseldorp, B. Blankert, A.J.B. Kemperman, J.C. Schippers, M.D. Kennedy, W.G.J. van der Meer, Application of a smart dosing pump algorithm in identifying real-time optimum dose of antiscalant in reverse osmosis systems, *J. Membr. Sci.* 658 (2022), 120717, <https://doi.org/10.1016/j.memsci.2022.120717>.
- [26] J.S. Vrouwenvelder, D. van der Kooij, Diagnosis, prediction and prevention of biofouling of NF and RO membranes, *Desalination* 139 (1) (2001) 65–71, [https://doi.org/10.1016/S0011-9164\(01\)00295-8](https://doi.org/10.1016/S0011-9164(01)00295-8).
- [27] L.A. Weinrich, E. Giraldo, M.W. LeChevallier, Development and application of a bioluminescence-based test for assimilable organic carbon in reclaimed waters, *Appl. Environ. Microbiol.* 75 (23) (2009) 7385–7390, <https://doi.org/10.1128/AEM.01728-09>.
- [28] A. Abushaban, S.G. Salinas-Rodriguez, N. Dhakal, J.C. Schippers, M.D. Kennedy, Assessing pretreatment and seawater reverse osmosis performance using an ATP-based bacterial growth potential method, *Desalination* 467 (2019) 210–218, <https://doi.org/10.1016/j.desal.2019.06.001>.
- [29] A. Abushaban, S.G. Salinas-Rodriguez, M. Philibert, L. Le Bouille, M.C. Necibi, A. Chehbouni, Biofouling potential indicators to assess pretreatment and mitigate biofouling in SWRO membranes: a short review, *Desalination* 527 (2022), 115543, <https://doi.org/10.1016/j.desal.2021.115543>.
- [30] L. Javier, N.M. Farhat, P. Desmond, R.V. Linares, S. Bucs, J.C. Kruithof, J. S. Vrouwenvelder, Biofouling control by phosphorus limitation strongly depends on the assimilable organic carbon concentration, *Water Res.* 183 (2020), 116051, <https://doi.org/10.1016/j.watres.2020.116051>.
- [31] S.F.E. Boerlage, M.D. Kennedy, M.R. Dickson, D.E.Y. El-Hodali, J.C. Schippers, The modified fouling index using ultrafiltration membranes (MFI-UF): characterisation, filtration mechanisms and proposed reference membrane, *J. Membr. Sci.* 197 (1–2) (2002) 1–21, [https://doi.org/10.1016/S0376-7388\(01\)00618-4](https://doi.org/10.1016/S0376-7388(01)00618-4).